

Xu Zheng · Meiling Wu · Fandong Kong ·  
Haihang Cui · Zhanhua Silber-Li

## Visualization and measurement of the self-propelled and rotational motion of the Janus microparticles

Received: 4 September 2014 / Revised: 30 March 2015 / Accepted: 19 April 2015 / Published online: 10 May 2015  
© The Visualization Society of Japan 2015

**Abstract** The self-propelled diffusiophoresis, induced by an asymmetric concentration gradient field, provides a new strategy to manipulate micro-objects (like some cells and colloids) in solutions. One example is the autonomous motion of the double-faced Janus microparticle (platinum coating on one half of a silica particle) due to a chemically catalyzed reaction (reduction of hydrogen peroxide) on the Pt surface. In this paper, a systematic method is developed to describe the details of self-propulsion and rotation of Janus microparticles, despite the difficulty induced by particle non-uniformity. From the measurement, we found that the particles presented a three-stage behavior of the dimensionless mean square displacement, and their displacement probability distribution formed a double-peaked structure. These results show the intrinsic characteristics and the non-Gaussian behavior of Janus particle's self-propulsion. Furthermore, the rotational motion is characterized by the rotational angle variation and the rotational diffusion coefficient. These results show that Brownian rotation still dominates the Janus microparticle's rotational motion, though the measured rotational diffusion coefficient presents an anomalous tendency.

**Keywords** Self-propulsion · Janus microparticle · Rotation

### 1 Introduction

In microfluidics, many applications could take advantage of the self-powered effect to propel micro/nano-scale objects (Golestanian et al. 2007; Marchetti et al. 2013; Soler et al. 2013). One strategy is to use the asymmetric concentration field around a double-faced Janus microparticle to drive its autonomous motion (Howse et al. 2007). This self-propulsion is also known as self diffusiophoresis. Taking the half-platinum half-silica (Pt-silica) Janus microparticle for example (Ebbens and Howse 2011), there is a catalytic reaction occurring on the Pt surface when the microparticle is put into hydrogen peroxide solution ( $\text{H}_2\text{O}_2$ ):  $2\text{H}_2\text{O}_2 \rightarrow 2\text{H}_2\text{O} + \text{O}_2$ . This decomposition of  $\text{H}_2\text{O}_2$  will generate more molecules and higher concentration on the Pt side, which converts chemical energy due to catalytic reaction into mechanical work, and thus

---

**Electronic supplementary material** The online version of this article (doi:[10.1007/s12650-015-0299-5](https://doi.org/10.1007/s12650-015-0299-5)) contains supplementary material, which is available to authorized users.

---

X. Zheng (✉) · Z. Silber-Li  
State Key Laboratory of Nonlinear Mechanics (LNM), Institute of Mechanics, CAS, Beijing 100190, China  
E-mail: zhengxu@lnm.imech.ac.cn

M. Wu · H. Cui  
Xi'an University of Architecture and Technology, Xi'an 710055, China

F. Kong  
Shanghai University, Shanghai 200444, China

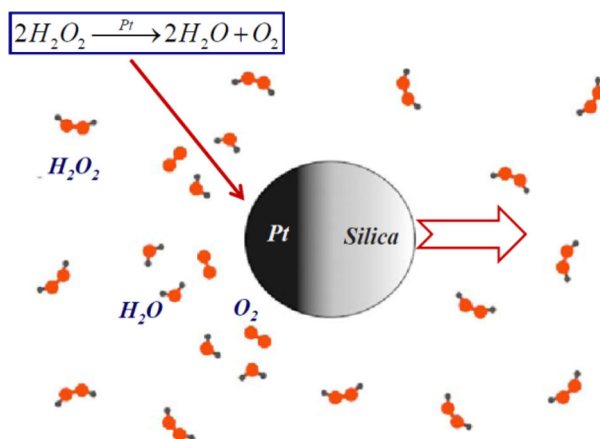


**Fig. 1** Schematic diagram of a self-propulsion of Pt-SiO<sub>2</sub> particle driven by decomposing H<sub>2</sub>O<sub>2</sub>

pushes the whole Janus microparticle to move to the other direction (Fig. 1). Owing to the advantages of the compact structure and no additional power supplier, self-propulsion of the Janus particle has attracted widespread attention. By means of microfluidic chips, this effect could offer an easy way to ferry cargos of specific cells or drug-loaded particles (Baraban et al. 2012; Paxton et al. 2006). Furthermore, it is of interest in biology to understand how some self-motile cells and bacteria utilize the concentration gradient in the environmental solution to swim (Elgeti et al. 2010; Chen et al. 2012). Therefore, this self-propelled Janus microparticle also provides a simple model to understand the swimming mechanism of microorganisms (Golestanian et al. 2007; Dreyfus et al. 2005).

Physically, the motion of Janus microparticle is a competition between the simple Brownian motion and the propulsion due to the concentration gradient. Previous studies have shown that the mean square displacement (MSD) presented a super-diffusive behavior at certain time intervals when self-propulsion dominated over Brownian motion (Howse et al. 2007; Ke et al. 2010; Ebbens et al. 2012). However, this result has not yet illustrated all the intrinsic behaviors of the self-propelled Janus microparticle (Wang and Wu 2014). On one hand, a full understanding about the translational MSD characteristic is still absent, and the dimensionless result is needed to illustrate the common behaviors of self-propulsion. Further, it has been argued that self-propulsion will cause Janus microparticle to disobey the rules of Gaussian Brownian motion and present significant non-Gaussian characteristics (ten Hagen et al. 2011). However, how to describe the difference between self-propulsion and simple Brownian motion remains unknown. On the other hand, the rotational motion which determines the moving direction of the microparticle has not been investigated in depth. Due to experimental difficulty, previous measurements only focused on the translational motion of Janus microparticles (Howse et al. 2007; Ke et al. 2010; Ebbens et al. 2012) and no experimental result about Janus microparticle's rotation has been reported. However, measuring the rotational behavior is of great interest, since it is one of the key factors in Janus microparticle's motion. For instance, whether the rotation is dominated by Brownian rotation or the eccentric moment due to the asymmetric propulsion is still an open question. Thus, the typical behaviors of both translational propulsion and rotation will be characterized, respectively, in this study.

In one of our previous studies, some non-Gaussian behaviors of the Janus microparticle's translational self-propulsion have been investigated (Zheng et al. 2013). In this paper, we will perform a thorough investigation of the Janus microparticle's motion. We first develop a systematic method to describe both the translational and rotational motions of the Janus microparticles. Compared to the previous experiment (Ke et al. 2010), our method can overcome the difficulty of determining the Janus particle's center due to its double-faced non-uniformity; it also provides an approach to measure the rotational motion of the Janus particle directly. Then by means of statistics, a full result will be presented to demonstrate the intrinsic behaviors of the translational motion and the characteristics of the rotational motion. We find that the dimensionless mean square displacement shows a three-stage behavior, and from the displacement probability distribution a double-peaked structure emerges, which has not been reported before. In Sect. 2, we will introduce the experimental setup and method. Special procedures of image processing which aim at tracking trajectories and obtaining the rotational angle of non-uniform double-faced microparticle are introduced. In Sect. 3, we present the results. Finally, the conclusions are given in Sect. 4.

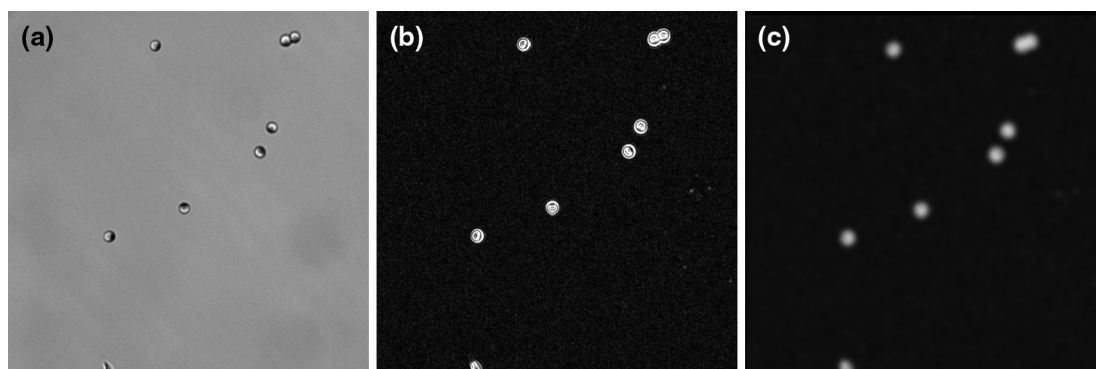


**Fig. 2** The image pre-process, **a** the original image, **b** image after “find edge” and **c** image after “Gaussian blur”

## 2 Experimental setup and method

In the experiments, the motion of spherical Pt–silica Janus microparticles was studied. Originally, we had monodispersed pure silica microspheres suspended in aqueous solution. To fabricate the Janus microparticle, the silica particles were first deposited on a 4-in. silicon wafer. By spin-coating, a monolayer of microparticles was formed on the wafer surface. By electron beam evaporation, a layer of Pt (thickness about 5–7 nm) was deposited on the surface of one hemisphere of the particles. After that the Janus microparticles were collected and re-suspended in distilled water (18.2 M $\Omega$  cm). The particle volumetric concentration (defined as the ratio between the volume of the particles and the volume of the solution) was approximately  $5 \times 10^{-3}$ , which is low enough to avoid over-intensive catalytic reaction that will induce excessive bubbles. Most of the experiments were performed with Janus spheres with diameter  $d_1 = 2.08 \pm 0.05 \mu\text{m}$  (measured by scanning electron microscopy); however, smaller particles with diameter  $d_2 = 0.96 \pm 0.03 \mu\text{m}$  were also included for comparison.

The particle motions in water and in H<sub>2</sub>O<sub>2</sub> solutions with different concentrations (1.25–15 %) were observed by video microscopy. An EMCCD (Andor 897) was used to capture videos with a 10 ms time interval  $\Delta t$  between two images. The exposure time of each frame was only 0.5 ms, which was much shorter than the interval  $\Delta t$ . This short time observation is very necessary to catch the particle dynamics. The image field of view was  $512 \times 512$  pixels (approximately,  $80 \times 80 \mu\text{m}$ ). After preparing the test solutions, a 70  $\mu\text{L}$  droplet with specified H<sub>2</sub>O<sub>2</sub> concentration was put on a glass coverslip. Image series consisting of about 1000 frames were recorded in one position located about 2–5  $\mu\text{m}$  above the glass substrate. The typical motion of Janus microparticle’s self-propulsion is shown in the supplementary video (the H<sub>2</sub>O<sub>2</sub> concentration were 2.5 and 10 % respectively).

The measurement should provide sufficient video materials for the subsequent statistical analysis. We thus design the measurement process as follows. In each droplet to be observed, five videos were taken in five different locations in the same horizontal plane. The measurements for each H<sub>2</sub>O<sub>2</sub> concentration were repeated in 12–15 droplets. To achieve good measurement reproducibility and limit the influence of temperature and concentration fluctuations induced by the chemical reaction, the fresh test solution was re-prepared for each droplet. The experiments were performed in the stationary regime from 1 to 9 min after the beginning of the catalytic reaction in the H<sub>2</sub>O<sub>2</sub> solution. In this period, the fuel H<sub>2</sub>O<sub>2</sub> concentration did not change significantly, since the particle volumetric concentration was very low. The displacements of the Janus particles were measured by trajectory tracking from the movies. To reach the requirements of the statistical analysis, more than 1000 particles and  $10^5$  displacements were measured for each concentration. The sampled amount was significantly larger than the previous experiments (Ke et al. 2010), which could guarantee the reliability of the statistical analysis performed.

In the images (Fig. 2a is the original image), the Janus particles appear half bright (the silica side) and half dark (Pt coating side). Obviously, the non-uniformity (double-faced) of the particle in the original image (Fig. 2a) could cause difficulty in trajectory tracking. The way in which to overcome this difficulty is to reconstruct the round and uniform particle domain and find the exact center of each Janus particle by image processing. To achieve that, a two-step method using the “find edge” and the “Gaussian blur” was performed. First, the find edge function of the program IMAGEJ was used (Fig. 2b), which would highlight sharp intensity changes. As the sharpest changes occurred at the particle edges, this function offered a way

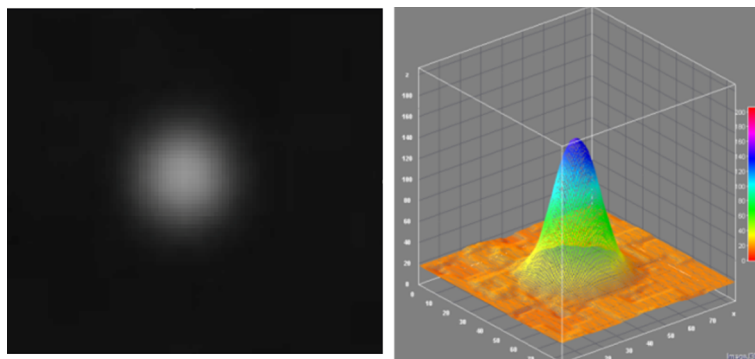


**Fig. 3** One particle domain after Gaussian blur (*left*), and its Gaussian grayscale value distribution (*right*)

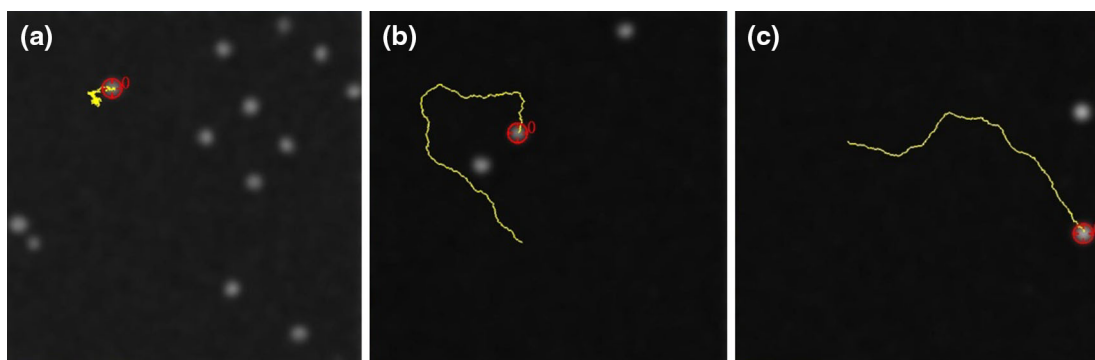


**Fig. 4** The typical trajectories of Janus particle movements in **a** water, **b** 5 %  $\text{H}_2\text{O}_2$  solution and **c** 10 %  $\text{H}_2\text{O}_2$  solution

to reconstruct the round shape of the particle. Secondly, using the Gaussian blur function of IMAGEJ, the Gaussian grayscale value distribution in the particle domain was established (Fig. 2c). Taking the particle located at the center of Fig. 2 as an example, the Gaussian distribution of the grayscale value can be seen after the above processing (Fig. 3). The point with the maximum grayscale value is considered to be the center of the particle. Thus, the center of the Janus particles could be determined with a  $\pm 0.5$  pixel precision. We would also like to emphasize the improvement of our method compared to the previous one (Ke et al. 2010), which only tracked the movement of the center of the bright side. Obviously, there was a relative motion/rotation of the bright side corresponding to the real particle center, which may lead to big error in measuring particle displacements.

After the pre-processing, the trajectories of individual particles could be tracked from the video by a free software called VIDEO SPOT TRACKER (V07.02, the trajectories are shown in Fig. 4). During the tracking process, the particle center positions ( $x$ ,  $y$ ) were recorded frame by frame by this software automatically. Figure 4 shows the typical trajectories of the Janus microparticle motion in different solutions. The red circle is the mark provided by the program to highlight the particles being tracked, and the yellow curve is the trajectory connecting the particle center positions of every frame. It is clear that the motion of the Janus microparticle in  $\text{H}_2\text{O}_2$  solution is significantly enhanced compared to simple Brownian motion in water. To make sure that only individual particles were tracked, the aggregated particles were not instructed in the program. Also, we used the “dead zone” function during the tracking, by which only the region of approximately one diameter around the particle was monitored. If other particles entered into this zone, the tracking of the respective particles was stopped. Therefore, particle aggregation as well as particle–particle collisions and interactions were excluded from our investigation.

To get rotation information, particle orientation should be determined first. The orientation angle  $\theta$  of the Janus microparticle is defined based on the vector  $\mathbf{AO}$  as shown in Fig. 5a.  $A$  is the geometric center of the dark half and  $O$  is the center of the whole spherical particle. The orientation angle  $\theta$  is the polar angle of  $\mathbf{AO}$  in polar coordinates. Thus, the rotational angle  $\alpha$  is obtained from the orientation angular change between two successive frames, which is calculated as  $\alpha = \theta_2 - \theta_1$ . Figure 5b shows how the orientation of a Janus microparticle changes in a time interval 2.15 s.

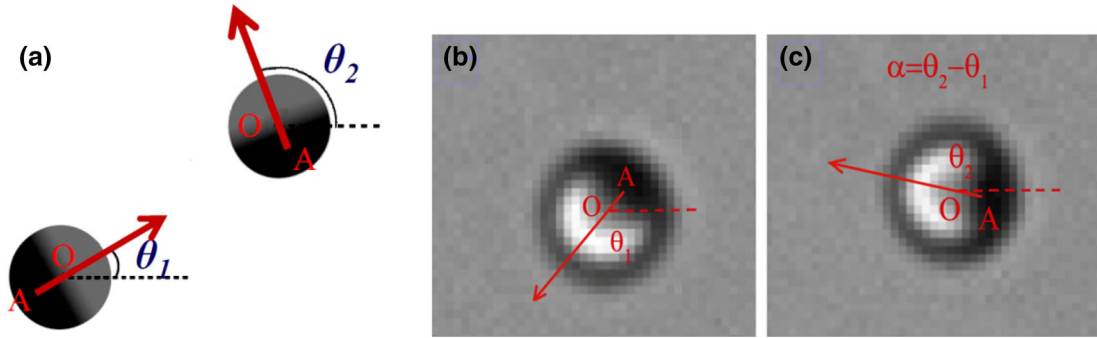


**Fig. 5** Schematic diagram of the orientation angle  $\theta$  of the Janus microparticle (a) and the experimental images of the orientation angular change in 2.15 s (b); the rotational angle  $\alpha$  is determined as  $\alpha = \theta_2 - \theta_1$

To get  $\theta$  from image processing, a similar method was used. The particle center  $O$  was obtained by the same method as mentioned above. We also re-constructed the Gaussian distribution of grayscale value in the dark half by the “Gaussian blur” function, and the darkest point was  $A$ . Therefore, the vector connecting the geometric center of the dark half  $A$  to the center of the whole particle  $O$  is established. Both  $A$  and  $O$  of every individual Janus microparticle were tracked separately by VIDEO SPOT TRACKER frame by frame. From the position of  $A$  and  $O$ ,  $\theta$  and  $\alpha$  could be calculated easily, and the angular range was set to be  $-180^\circ \leq \theta, \alpha < 180^\circ$ . Theoretically, the uncertainty of rotational angle can be estimated as follows: The length of vector  $AO$  is about 4 pixels, and the uncertainty of determining the position of  $O$  or  $A$  is smaller than 0.5 pixels. So the uncertainty of the orientation angle  $\theta$  is smaller than  $\arctan(0.5/4) \approx 7.1^\circ$ . Considering that the rotational angle is  $\alpha = \theta_2 - \theta_1$ , we estimate that the uncertainty of the rotational angle  $\alpha$  should be approximately  $5^\circ$ – $10^\circ$ . In the experiment, we also examined the precision of this method and found the uncertainty of rotational angle  $\alpha$  to be limited within  $10^\circ$  when  $2 \mu\text{m}$  Janus particles were used.

### 3 Results

#### 3.1 Mean square displacement $\langle L^2 \rangle$

By tracking the particle trajectories and calculating the displacements, the measured MSD  $\langle L^2 \rangle$  is obtained. Figure 6 shows the measured MSD of 2 and 1  $\mu\text{m}$  Janus microparticles. The solid lines and the dashed lines in Fig. 6a are the results of two independent measurements, which show very good agreement and reproducibility. For 2  $\mu\text{m}$  Janus microparticles (Fig. 6a), its MSD in Di-water follows a linear increase  $\langle L^2 \rangle \sim t$ , because there is only Brownian motion. However, in  $\text{H}_2\text{O}_2$  solutions, the measured MSD increases nonlinearly at the beginning ( $t \approx 0$ –5 s), and after that the increase becomes linear again. For 1  $\mu\text{m}$  Janus microparticles (Fig. 6b), a similar tendency can be observed: the measured MSD increases nonlinearly up to approximately 0.5 s and shows a linear increase afterward. All the measured curves indicate a transition from a nonlinear increase at short times to a linear increase at long times.

Further, we find that the transition time is close to the typical rotational time scale  $\tau_r$  based on the inverted rotational diffusion coefficient  $D_r$ :

$$\tau_r = \frac{1}{D_r} = \frac{\pi \mu d^3}{k_B T}, \quad (1)$$

where  $\mu$  is the fluid viscosity,  $d$  the Janus sphere diameter and  $k_B T$  the thermal energy. For 2  $\mu\text{m}$  Janus microparticles,  $\tau_r = 6.7$  s; and for 1  $\mu\text{m}$  Janus microparticles,  $\tau_r = 0.65$  s. Since this typical time scale  $\tau_r$  can distinguish different behaviors of motion, the dimensionless results can be given by the defined  $z^+ = \langle r^2 \rangle / d^2$  and  $\tau = t / \tau_r$ . Figure 7 shows the variation of dimensionless MSD with dimensionless time. More than what we can see from Fig. 6, a three-stage behavior is revealed in Fig. 7 (Zheng et al. 2013):

- (I) The first stage is at short times of about  $\tau < 0.01$ . The dimensionless MSD measured in different  $\text{H}_2\text{O}_2$  solutions is similar to the tendency of Brownian motion in DI-water. The concentration gradient caused by catalytic reaction has not been established as the time is not sufficient. The particle motion is still dominated by Brownian motion. The end time  $\tau \sim 0.01$  is used to quantify the typical time scale of the

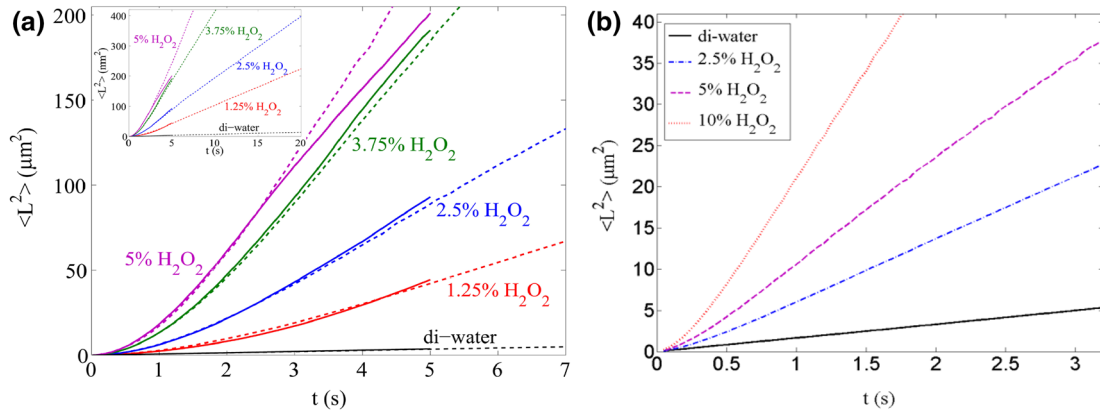


**Fig. 6** The measured MSD versus time, **a** the curves of  $d_1 = 2 \mu\text{m}$  particles; **b** the curves of  $d_2 = 1 \mu\text{m}$  particles. The *inset* in **(a)** is the long-time variation of MSD up to 20 s

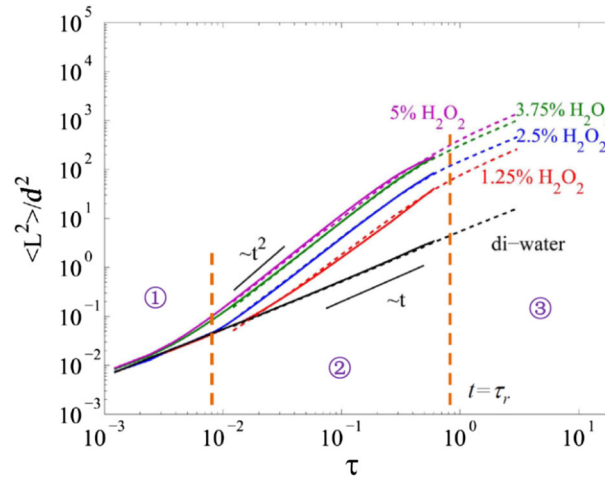


**Fig. 7** The three-stage dimensionless MSD. The slopes of  $t$  and  $t^2$  are given for comparison. The three stages separated by the orange dashed lines are also marked in this figure

decomposition of  $\text{H}_2\text{O}_2$ . At higher  $\text{H}_2\text{O}_2$  concentration (like the purple curve of 5 %  $\text{H}_2\text{O}_2$  in Fig. 7), the measured curve starts deviating from the earlier linear tendency.

- (II) The second stage is at an intermediate time around  $0.01 < \tau < 1$ . In this stage, “self-propulsion” dominates and thus results in a nonlinear increase of dimensionless MSD. The slopes of the increasing curves in different  $\text{H}_2\text{O}_2$  solutions also follow  $t^2$ , indicating a so-called super-diffusive behavior (ten Hagen et al. 2011).
- (III) The third stage is at long times  $\tau > 1$ . In this stage, the dimensionless MSD measured in different  $\text{H}_2\text{O}_2$  solutions shows a linear relation with time again; thus their behavior is called Brownian-like (Howse et al. 2007). Nevertheless, the absolute values of the MSD in different  $\text{H}_2\text{O}_2$  solutions are several orders larger than that measured in DI-water, which shows the mobility enhancement of the self-propelled Janus microparticle. The transition from stage (II) to stage (III) locates right at  $\tau = 1$  ( $t = \tau_r$ ), implying the contribution of particle rotation is also important to characterize the Janus microparticle movement.

This is the first time that the full three-stage behavior has been reported by our experiment. The results show clearly that the transition from self-propulsion (stage II) to Brownian-like motion (stage III) occur right at about  $\tau = 1$ , no matter what sizes of particles and what concentrations of  $\text{H}_2\text{O}_2$  solutions were used. It differs from the previous results (Howse et al. 2007; Ke et al. 2010) that showed the transition time was concentration dependent. One explanation of this difference might be that the sampled number of particles in the previous measurement was not sufficient for statistics; therefore their data were still scattered. Besides

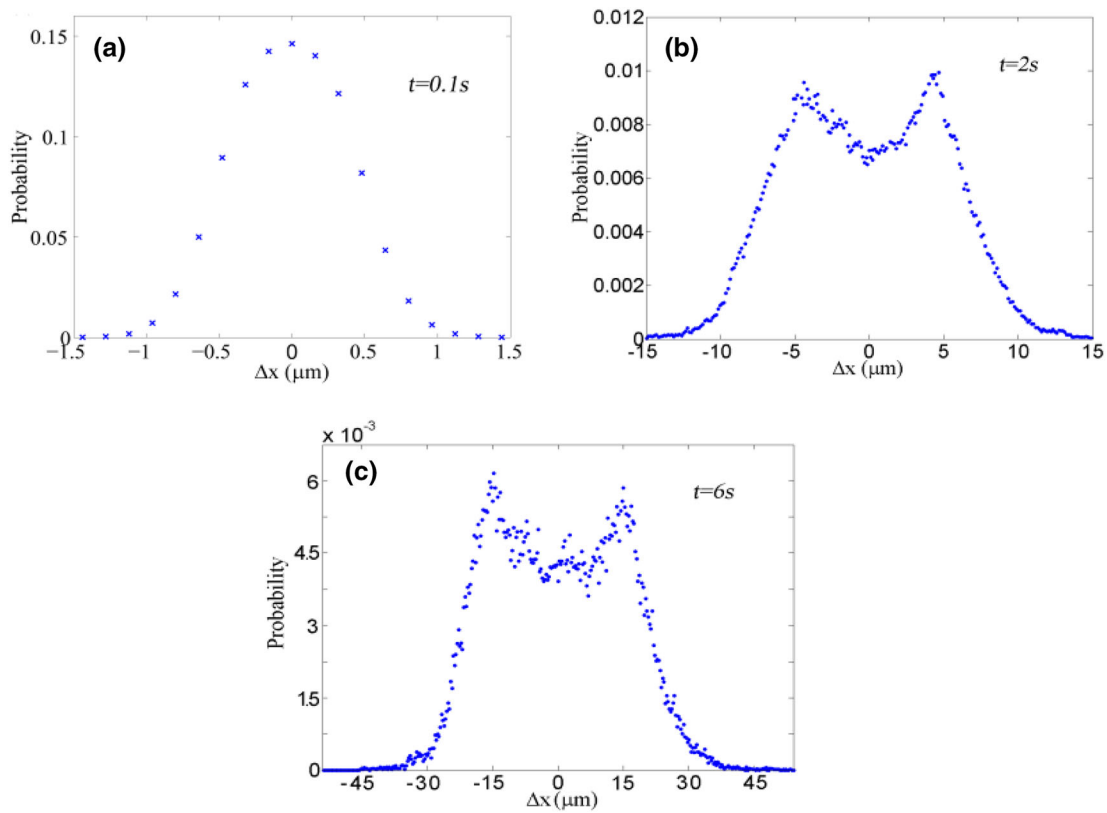


**Fig. 8** The measured probability distribution of  $\Delta x$  in 10 %  $\text{H}_2\text{O}_2$  solution at different times **a**  $t = 0.1$  s, **b**  $t = 2$  s, and **c**  $t = 6$  s

that, we can also observe that the slopes of the dimensionless MSD curves in Fig. 7 always follow  $t^2$ , which is a typical signal of the propulsion force.

### 3.2 Displacement probability distribution (DPD)

It is of great interest to show how particle self-propulsion influences the displacement probability distribution (DPD). The DPD offers an alternative way to characterize the translational motion of Janus microparticles. Take the motion of the Janus microparticle in 10 %  $\text{H}_2\text{O}_2$  solution as an example, Fig. 8 shows the measured probability distribution of displacement  $\Delta x$ . At the beginning (Fig. 8a,  $t = 0.1$  s), the DPD is still Gaussian as Brownian motion is dominant, since it is still in the short time stage. However, as time increases, the double-peaked structure emerges clearly (Fig. 8b, c). This special characteristic that indicates the intrinsic non-Gaussian behavior of the self-propelled motion has never been reported in previous studies. The emergence of the double peaks can be understood as the consequence of the deterministic displacement due to the directional self-propulsion. Compared to the simple Brownian motion, the self-propulsion results in directed displacement, which could break Gaussian distribution. Considering the initial orientations of the Janus particles which are homogeneously distributed on a unit circle located on the plane, we observed that the corresponding displacement projections on the  $x$  axis were not evenly spread between  $-1$  and  $1$ . Instead of that, values close to the extrema have a higher statistical contribution than the values around zero due to self-propulsion. Therefore, the double peaks in Fig. 8 show the most probable directed displacements, which could offer interesting information in microfluidics when people want to manipulate Janus microparticles.

We also measured the DPD (both  $\Delta x$  and  $\Delta y$ ) of  $2 \mu\text{m}$  Janus microparticles in different  $\text{H}_2\text{O}_2$  solutions. Figure 9 directly visualizes the measured DPD of different concentrations at a certain time  $t = 2$  s. The insets in Fig. 9 show the measured DPD of simple Brownian motion in water, in which Gaussian distribution can be still observed. However, in the  $\text{H}_2\text{O}_2$  solutions, the double-peaked structure can be clearly observed. This double-peaked structure is much more obvious in higher  $\text{H}_2\text{O}_2$  concentration solutions. This tendency

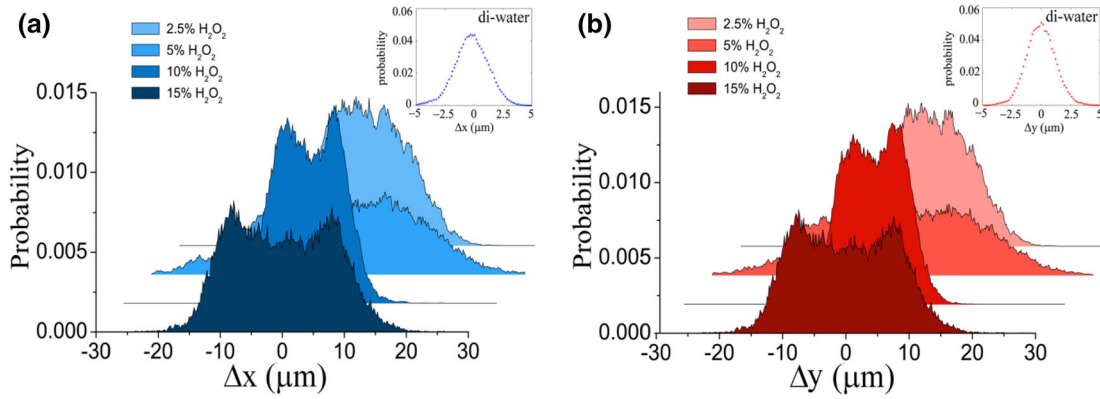


**Fig. 9** The measured DPD in different  $\text{H}_2\text{O}_2$  solutions, **a**  $\Delta x$  and **b**  $\Delta y$

also indicates that the double-peaked structure is related to the directed displacement which becomes more significant in a solution with higher  $\text{H}_2\text{O}_2$  concentration.

### 3.3 Rotational angle and rotational diffusion coefficient

Besides the translational motion described above, we also try to characterize the rotational motion of the Janus microparticle. One interesting phenomenon observed in the experiments is the change of rotation mode in different solutions. We found that in DI-water or in diluted  $\text{H}_2\text{O}_2$  solutions (concentration is smaller than 5 %, see Fig. 10a), the particle rotation is three dimensional. This means the particle orientation angle  $\theta$  could sometimes point to the out-of-plane direction, as shown in sub-images 4 and 5 in Fig. 10a. However, in  $\text{H}_2\text{O}_2$  solutions with concentration larger than 5 % (Fig. 10b), we always found that the Janus particle appeared approximately half-bright half-dark, and the orientation vector stayed in the horizontal plane. One possible explanation could be the confinement effect of the substrate (Gauger and Stark 2006; Gotze and Gompper 2010). It is argued that the hydrodynamic effect due to the presence of substrate could limit the rotation freedom. Some details can be found in our previous studies published elsewhere (Wu et al. 2014), which showed significant influence on the concentration gradient and the driving force near the substrate wall.

We then measured the rotational angle probability distribution at different time intervals ( $t = 0.05, 1, 5, 10, 15$  and  $17$  s) in different solutions. In DI-water (Fig. 11a), at  $t = 0.05$  s, the probability distribution is Gaussian, the rotational angle mainly concentrates in the range  $(-40^\circ, 40^\circ)$ , and the peak probability value is about 0.34. Then, with the increase of  $t$ , the rotational angle distribution becomes wider. Finally, when  $t > 15$  s approximately, the probability of rotational angle at all values are equal. This result describes well the simple Brownian rotation of the microparticle.

In  $\text{H}_2\text{O}_2$  solutions, although the distributions are similar to those in DI-water, some differences still exist, especially at short times (Fig. 11b–d). When  $t = 0.05$  s, in 2.5–5 %  $\text{H}_2\text{O}_2$  solutions, the peak probability increases from 0.34 to 0.36, and the peak width decreases from  $(-40^\circ, 40^\circ)$  to approximately  $(-30^\circ, 30^\circ)$ . If the concentration further increases to 10 %, the peak value goes up to 0.4 as well and the width turns narrower to  $(-25^\circ, 25^\circ)$ . The reason is that at higher concentration, the propelled force is stronger so that the Janus microparticle presents a stronger directional motion rather than rotation. However, this effect is not strong enough compared to the result of simple Brownian rotation shown above. At longer times, the Brownian rotation always flattens the angle distribution and eliminates the influence of directional motion. Therefore, the Brownian rotation is still accounted for as the dominant effect of the Janus microparticle's rotational motion.

By measuring the rotational angle, it is also possible to calculate the rotational diffusion coefficient  $D_r$  based on:

$$\langle s^2 \rangle = 4D_r t, \quad (2)$$

where  $s$  is the length of arc corresponding to the rotational angle. The measured rotational diffusion coefficients  $D_r$  in different solutions are shown in Fig. 12. It can be seen from the figure that at short times,  $D_r$  of Janus microparticle has a larger value and it decreases rapidly. As observation time interval increases,

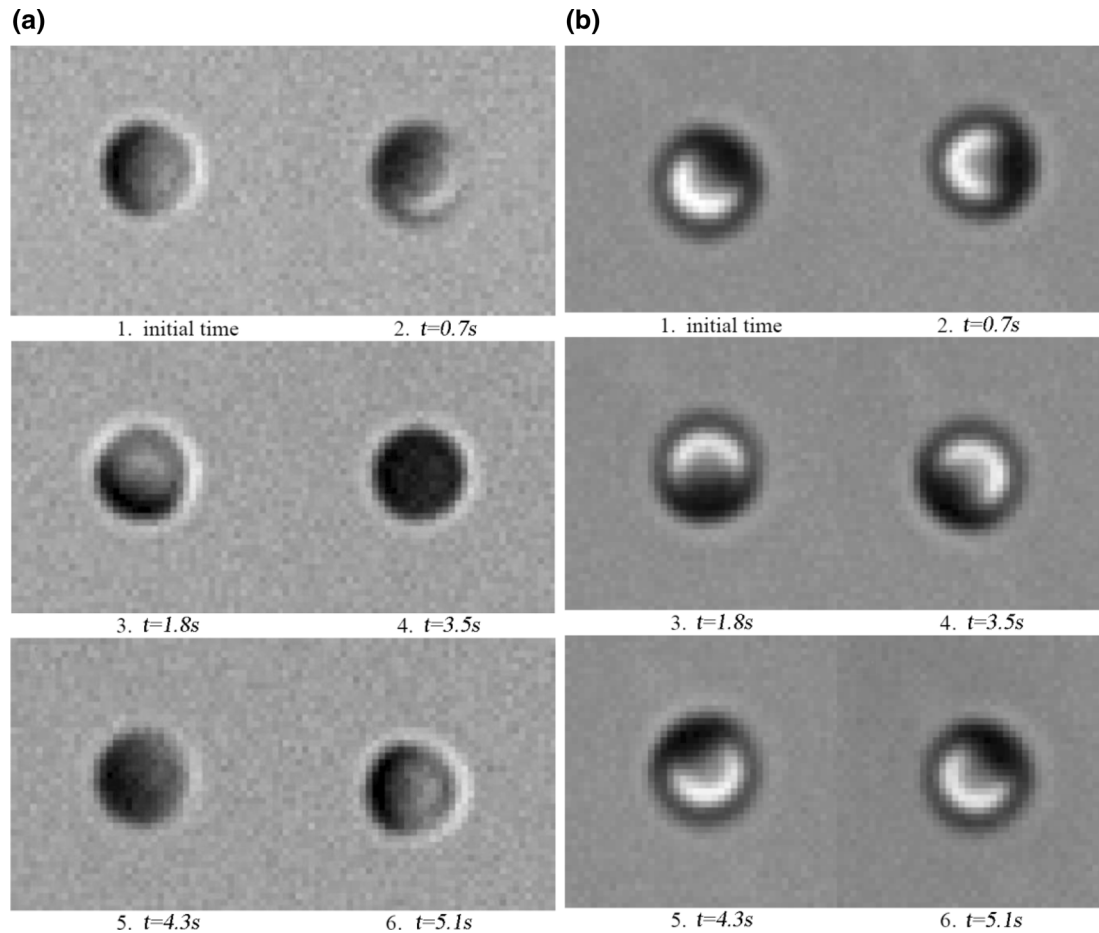


**Fig. 10** The snapshots of the orientation of 2  $\mu\text{m}$  Janus microparticle in **a** DI-water and **b** 10 %  $\text{H}_2\text{O}_2$  solution

$D_r$  turns to a constant value of about  $D_r = 0.079 \text{ s}^{-1}$ . The influence of  $\text{H}_2\text{O}_2$  concentration is also clear. At most times, the measured  $D_r$  in  $\text{H}_2\text{O}_2$  solutions is smaller than that in DI-water, and the measured value of  $D_r$  decreases with the increase of  $\text{H}_2\text{O}_2$  concentration. We think the explanations could be as follows. Firstly, since the Janus microparticle prefers the directional motion in  $\text{H}_2\text{O}_2$  solution, it presents a narrower distribution of rotational angle and results in smaller measured  $D_r$ . Secondly, as mentioned earlier in this section, the confinement effect becomes stronger at higher  $\text{H}_2\text{O}_2$  concentration (Gauger and Stark 2006; Gotze and Gompper 2010; Wu et al. 2014), which could limit the angular change of the Janus microparticle when  $\text{H}_2\text{O}_2$  concentration is larger than 5 %.

When we take the long-time constant value as the effective rotational diffusion coefficient, we get approximately  $D_r = 0.079 \text{ s}^{-1}$ . However, according to Eq. (1), the theoretical value of  $D_r$  can be calculated to be  $0.149 \text{ s}^{-1}$ , which is two times larger than the measured value. It is surprising that even in water, where there is no self-propulsion, the measured value of  $D_r$  is still much smaller than the theoretical value. Thus, there should be other hydrodynamic effect influencing the particle rotation near wall, except for the propulsion due to chemical reaction analyzed in this study. The reason for this anomalous deviation needs further investigation.

#### 4 Conclusions

In summary, this paper examines the self-propelled motion and rotation of Pt-silica Janus particle experimentally. The experiments were performed using both  $\phi 2 \mu\text{m}$  and  $\phi 1 \mu\text{m}$  particles in DI-water or in  $\text{H}_2\text{O}_2$  solutions with different concentrations (1.25–15 %). We improve the measurement technique and image processing method to capture the major characteristics of self-propulsion and rotation. Our

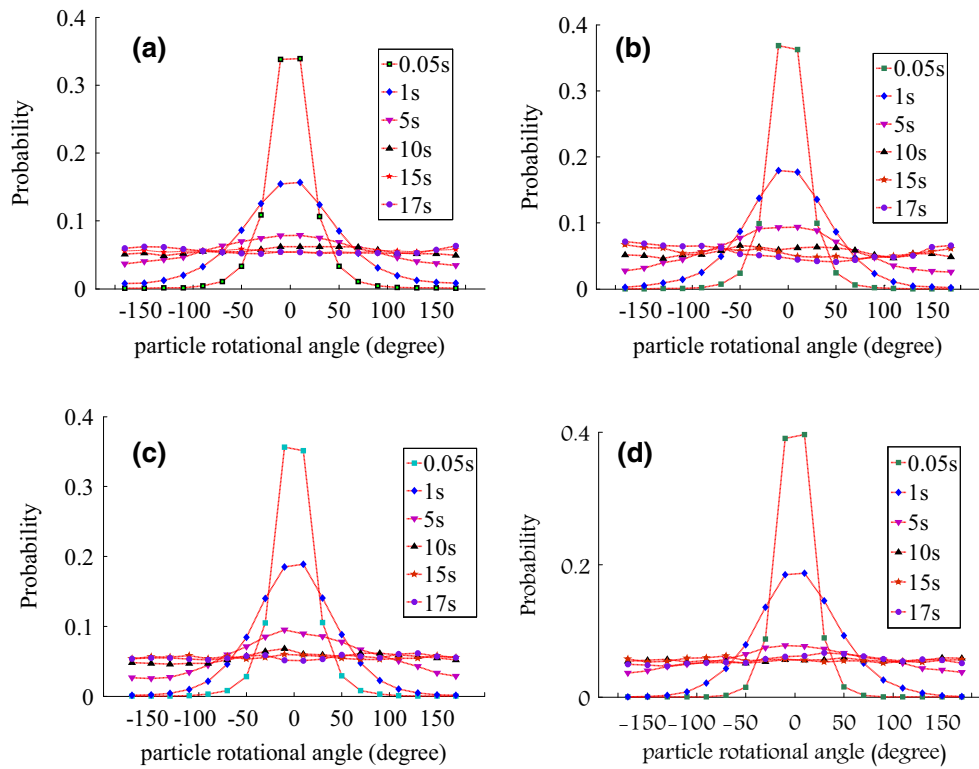


**Fig. 11** The temporal variation of rotational angle probability distribution in different solutions. **a** DI-water, **b** 2.5 %  $\text{H}_2\text{O}_2$ , **c** 5 %  $\text{H}_2\text{O}_2$ , **d** 10 %  $\text{H}_2\text{O}_2$

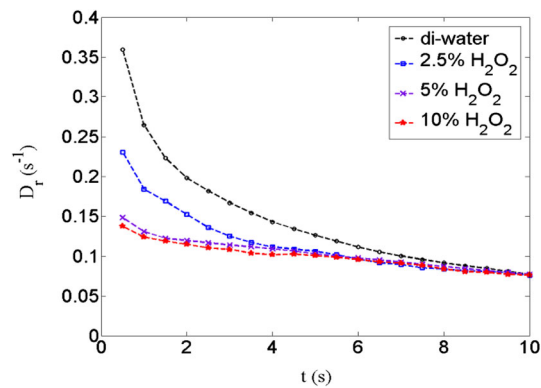


**Fig. 12** The measured rotational diffusion coefficient  $D_r$

experiment shows that the whole movement of the Janus microparticle can be considered as a combination of the translational self-propulsion and the rotational motion. The detailed result of this study could offer important information for the microfluidic applications manipulating the Janus microparticles. The main results include:

1. Three different stages of motion were observed: the Janus particle shows simple Brownian motion at short times, then self-propelled due to diffusiophoresis at intermediate times, and finally presents Brownian-like motion again at long times. The typical rotational time  $\tau_r$  is found to be the transition time scale between stage two and three. The transition always occurs at  $\tau = 1$  independent of the particle size and the  $\text{H}_2\text{O}_2$  concentration. Also, the slopes of the dimensionless MSD curves in the self-propelled stage always follow  $t^2$ .

2. The displacement probability distribution shows double-peaked structure due to self-propulsion, which also illustrates the non-Gaussian behavior of Janus microparticles.
3. The rotation angle variation and the rotational diffusion coefficient were also measured to characterize the rotational motion. The Brownian rotation is still considered to be the dominating effect of the Janus microparticle's rotational motion. The anomalous deviation between the measured rotational diffusion coefficient and the theoretical value of a Brownian particle is observed. We find that the presence of substrate wall and the near wall hydrodynamic effect could affect the particle rotation significantly.

**Acknowledgments** This work was financially supported by the National Natural Science Foundation of China (Grants No. 11272322, No. 11202219, and No. 21005058). The authors are very grateful for the discussion with Dr. ten Hagen and Prof. Löwen.

## References

- Baraban L, Makarov D, Steubel R, Mönch I, Grimm D, Sanchez S, Schmidt OG (2012) Catalytic Janus motors on microfluidic chip: deterministic motion from targeted cargo delivery. *ACS Nano* 6(4):3383–3389
- Chen X, Dong X, Be'er A, Swinner H, Zhang HP (2012) Scale-invariant correlations in dynamic bacterial clusters. *Phys Rev Lett* 108:148101
- Dreyfus R, Baudry J, Roper ML, Fermigier M, Stone HA, Bibette J (2005) Microscopic artificial swimmers. *Nature* 437:862
- Ebbens SJ, Howse JR (2011) Direct observation of the direction of motion for spherical catalytic swimmers. *Langmuir* 27:12293–12296
- Ebbens S, Tu MH, Howse JR, Golestanian R (2012) Size dependence of the propulsion velocity for catalytic Janus-sphere swimmers. *Phys Rev E* 85:020401(R)
- Elgeti J, Kaupp UB, Gompper G (2010) Hydrodynamics of sperm cells near surfaces. *Biophys J* 99(4):1018–1026
- Gauger E, Stark H (2006) Numerical study of a microscopic artificial swimmer. *Phys Rev E* 74:021907
- Golestanian R, Liverpool TB, Ajdari A (2007) Designing phoretic micro- and nano-swimmers. *New J Phys* 9:126
- Gotze I, Gompper G (2010) Mesoscale simulations of hydrodynamic squirmer interactions. *Phys Rev E* 82:041921
- Howse JR, Jones RAL, Ryan AJ, Gough T, Vafabakhsh R, Golestanian R (2007) Self-motile colloidal particles: from directed propulsion to random walk. *Phys Rev Lett* 99:048102
- Ke H, Ye SR, Carroll RL, Showalter K (2010) Motion analysis of self-propelled Pt-Silica particles in hydrogen peroxide solutions. *J Chem Phys* 114:5462
- Marchetti MC, Joanny JF, Ramaswamy S, Liverpool TB, Prost J, Rao M, Simha RA (2013) Hydrodynamics of soft active matter. *Rev Mod Phys* 85:1143
- Paxton WF, Sundararajan S, Mallouk TE, Sen A (2006) Chemical locomotion. *Angew Chem Int Ed* 45:5420–5429
- Soler L, Magdanz V, Fomin VM, Sanchez S, Schmidt OG (2013) Self-propelled micromotors for cleaning polluted water. *ACS Nano* 7(11):9611–9620
- ten Hagen B, van Teeffelen S, Löwen H (2011) Brownian motion of a self-propelled particle. *J Phys Condens Matter* 23:194119
- Wang S, Wu N (2014) Selecting the swimming mechanisms of colloidal particles: bubble propulsion versus self-diffusiophoresis. *Langmuir* 30(12):3477–3486
- Wu ML, Zhang H, Zheng X, Cui HH (2014) Simulation of diffusiophoresis force and the confinement effect of Janus particles with the continuum method. *AIP Adv* 4:031326
- Zheng X, ten Hagen B, Kaiser A, Wu ML, Cui HH, Silber-Li ZH, Löwen H (2013) Non-Gaussian statistics for the motion of self-propelled Janus particles: experiment vs. theory. *Phys Rev E* 88:032304